Received: 26 September 2025 | Revised: 16 March 2026 | Accepted: 2 April 2026

DOI: 10.1002/alz.71463

Alzheimer's & Dementia®
THE JOURNAL OF THE ALZHEIMER'S ASSOCIATION

RESEARCH ARTICLE

Single-cell transcriptomic analysis reveals *APOE* genotype-dependent sex differences in Alzheimer's disease

Gefei Yu[1,2] | **Abigail Thorpe**[1,2] | **Qi Zeng**[1,2] | **Erming Wang**[1,2] | **Alison Goate**[1,3] | **Dongming Cai**[4,5,6] | **Minghui Wang**[1,2,7] | **Bin Zhang**[1,2,7,8]

[1]Department of Genetics and Genomic Sciences, Icahn School of Medicine at Mount Sinai, New York, New York, USA

[2]Mount Sinai Center for Transformative Disease Modeling, Icahn School of Medicine at Mount Sinai, New York, New York, USA

[3]Ronald M. Loeb Center for Alzheimer's Disease, Icahn School of Medicine at Mount Sinai, New York, New York, USA

[4]Department of Neurology, University of Minnesota, Minneapolis, Minneapolis, USA

[5]N. Bud Grossman Center for Memory Research and Care, University of Minnesota, Minneapolis, Minneapolis, USA

[6]Geriatric Research Education and Clinical Center (GRECC), Minneapolis VA Health Care System, Minneapolis, Minneapolis, USA

[7]Icahn Genomics Institute, New York, New York, USA

[8]Department of Pharmacological Sciences, Icahn School of Medicine at Mount Sinai, New York, New York, USA

Correspondence
Bin Zhang and Minghui Wang, Department of Genetics and Genomic Sciences, Icahn School of Medicine at Mount Sinai, One Gustave L. Levy Place, New York, NY, 10029, USA.
Email: bin.zhang@mssm.edu and minghui.wang@mssm.edu

Funding information
National Institutes of Health, Grant/Award Numbers: RF1AG054014, R56AG058655, RF1AG074010, UO1AG046170, RF1AG057440, RO1AG057907, R21AG077168, RF1AG077828; Alzheimer's Association, Grant/Award Number: AARG-22-928419

Abstract

INTRODUCTION: Alzheimer's disease (AD) is the most common form of dementia, with approximately two-thirds of AD patients being female. Basic and clinical research studies provide strong evidence that sex-specific differences contribute to AD complexity. Additionally, sex-specific interactions between apolipoprotein E (*APOE*) $\varepsilon 4$, the primary genetic risk factor of AD, and AD-associated neurodegenerative processes are well documented. However, there has been no comprehensive investigation into the interplay between sex and *APOE* genotypes at the single-cell level.

METHODS: In this study, we systematically explore sex- and *APOE*-associated differences in single-cell transcriptomics in AD.

RESULTS: Our work provides a high-resolution landscape of sex and *APOE* genotype-specific transcriptomic changes across 54 high-resolution cell types in AD and highlights genes and brain cell populations that show significant sex- and *APOE*-specific differences in AD.

DISCUSSION: This study lays the groundwork for understanding the complex molecular mechanisms of AD and informs the development of targeted sex- and *APOE*-stratified interventions for AD.

KEYWORDS
Alzheimer's disease, apolipoprotein E, *APOE*, sex difference, single cell, transcriptomics

Highlights

- *APOE* genotype-specific and sex-specific differences contribute to the complexity of AD.
- Characterization of the interplay between sex and APOE genotypes at the single-cell transcriptomic level can unravel the molecular mechanisms underlying AD pathogenesis.
- A novel similarity metric, the Zhang-Yu similarity measure was devised to efficiently identify shared and divergent transcriptional patterns across cell types, sexes, and *APOE* genotypes in over 640 *post mortem* brain samples.

- Our study highlights genes and pathways underlying sex- and *APOE*-associated transcriptomic changes across 54 high-resolution cell types in AD brains.

1 | BACKGROUND

Alzheimer's disease (AD) is the most prevalent neurodegenerative disorder of aging,[1] with approximately two-thirds of AD patients being female.[2] There are conflicting reports in the literature regarding the incidence of AD among males and females, with some reports suggesting a higher incidence of AD in females than males and others suggesting no differences.[3–7] Evidence from basic and clinical research studies supports sex-specific differences contributing to the complexity of AD. For example, sex-biased changes in brain structures and connectome have been demonstrated in AD subjects using various neuroimaging modalities. These studies found that the rates of brain atrophy in females were 1% to 1.5% faster than those in males, most prominently seen in those with mild cognitive impairment (MCI), with a 1% increase in atrophic rates and 2% in ventricular expansion.[8] Sex-specific brain region atrophy has also been reported.[9] Moreover, a significantly higher reduction of hippocampal integrity in female AD subjects was reported compared to male subjects through magnetic resonance imaging studies of the Minimal Interval Resonance Imaging in Alzheimer's Disease database.[10]

There is strong evidence supporting sex-specific interactions between apolipoprotein E (*APOE*) ε4, the primary genetic risk factor of AD, [11] and neurodegenerative processes associated with AD.[12,13] For example, sex modified the effects of *APOE* ε4 allele on region specific tau deposition and atrophy in AD.[14] Females exhibited a stronger association between *APOE* ε4 and cerebrospinal fluid (CSF) tau levels in amyloid-positive individuals.[15,16] There was a stronger association of *APOE* ε4 with cortical thinning, volume loss, brain connectivity, and hypo-metabolism in females than in males.[17–19] Moreover, females presented stronger associations of *APOE* ε4 with cognitive impairment, memory decline, and neuropsychiatric symptoms of AD.[20,21] On the other hand, male-specific associations with cerebral amyloid angiopathy (CAA) and microbleeds in AD have been reported.[22] Yet little has been done to understand the interplay between *APOE* and sex in aging and AD.

To address this gap, several transcriptomic studies have recently emerged. Bulk RNA sequencing (RNA-seq) of aged human brain from the Aging, Dementia and Traumatic Brain Injury Study revealed that female *APOE* ε4 carriers showed a much larger set of *APOE*-correlated genes than male *APOE* ε4 carriers.[23] They also identified specific genes with sex–*APOE* interaction effects, including *CNTNAP2*, a neurexin family member, and *PSEN2*, a known AD risk gene.[23] Besides human tissues, studies in model systems also discovered *APOE* ε4's distinctive role in a sex-specific manner. Moser et al. demonstrated in an *APOE*-familial AD (FAD) mouse model that microglial gene expression changes associated with *APOE* ε4 were amplified in females and that, even in the absence of AD, the presence of *APOE* ε4 and female sex might increase amyloid beta (Aβ) accumulation through transcriptional alterations affecting microglial function.[24] Sex-specific immune alterations have also been identified through network-based analysis and cell type deconvolution. Paranjpe et al. reported that female patients exhibited a unique *APOE* ε4 associated dysregulation of zinc finger nuclease genes, metabolic changes, and immune cell composition shifts, all of which were absent in male patients.[25] Similarly, stratified serum analyses have uncovered metabolic alterations unique to *APOE* ε4 females.[26] Recently, we systematically identified sex- and *APOE* ε4-specific differentially expressed genes (DEGs) in AD[27] using the bulk tissue RNA-seq data of *post mortem* human brain samples from the Mount Sinai Brain Bank (MSBB) cohort[28] and the Religious Orders Study and Rush Memory and Aging Project (ROSMAP) cohort.[29] We further developed sex-specific gene network models of AD to predict sex-specific driver genes and subsequently validated lipoprotein receptor-related protein 10 (*LRP10*) as a female-specific driver of AD pathogenesis, which has increased expression in *APOE* ε4 females but not in *APOE* ε4 males.[27]

In this study, we investigate the interplay between sex and *APOE* in AD at the single-cell level through differential gene expression analysis of single-nucleus RNA-seq (snRNA-seq) data. The findings not only provide a comprehensive overview of sex- and *APOE* genotype-specific transcriptomic changes across 54 high-resolution cell types in AD but also highlight individual genes and brain cell types that show significant differences between sexes and *APOE* genotypes. This study lays the groundwork for exploring the complex molecular mechanisms of AD and will inform the development of effective sex- and *APOE*-stratified interventions for AD.

2 | METHODS

2.1 | Dataset

To investigate the genes, pathways, and cell types underlying the sex and *APOE* isoform differences in AD pathology, we leveraged one of the most comprehensive snRNA-seq datasets in AD research by Mathys et al.[30] This dataset includes 2.3 million nuclei isolated from the prefrontal cortex of 427 participants in the ROSMAP cohort and spans a wide range of AD progression. Based on the final consensus cognitive diagnosis score (cogdx), participants were categorized as no cognitive impairment (NCI; cogdx = 1; n = 144), MCI (cogdx = 2; n = 102), AD (cogdx = 4; n = 146), and other dementia (cogdx = 3, 5, or 6; n = 35).

We used preprocessed read count data from the original study, which identified 54 high-resolution cell types grouped into 12 major

RESEARCH IN CONTEXT

1. **Systematic review**: The authors reviewed the literature using PubMed. While there have been several recent publications describing either sex- or *APOE*-associated transcriptomic changes in AD, the molecular mechanisms underlying *APOE* genotype- and sex-specific difference in AD are not yet fully understood.
2. **Interpretation**: Our findings lead to a high-resolution landscape of sex- and *APOE* genotype-specific transcriptomic changes across 54 high-resolution cell types in AD, providing insights into the development of targeted, sex- and *APOE*-stratified interventions for AD.
3. **Future directions**: The manuscript identifies novel targets for future studies for their potential roles in the complex interplays between sex and *APOE* genotypes in the context of AD-related transcriptional responses. Examples include (a) in silico validation of targets from additional large-scale snRNA-seq of AD when available; (b) experimental validation and characterization of functional roles of the target genes in a sex- and *APOE*-specific manner in relevant cell type-specific models; and (c) predicting and testing molecular compounds for sex- and *APOE*-specific interventions of the targets.

TABLE 1 Cohort characteristics and cell composition.

A. Number of samples used in this study as stratified by sex and APOE genotype combinations (ε2x = ε2/ε2 or ε2/ε3; ε33 = ε3/ε3; ε4x = ε3/ε4 or ε4/ε4).	
Sex–*APOE* group	**Number of samples**
Female *APOE* ε2 carriers (F_ε2x)	25 (8 AD; 17 NCI)
Female *APOE* ε3/ε3 genotypes (F_ε33)	82 (37 AD; 45 NCI)
Female *APOE* ε4 carriers (F_ε4x)	37 (26 AD; 11 NCI)
Male *APOE* ε2 carriers (M_ε2x)	13 (7 AD; 6 NCI)
Male *APOE* ε3/ε3 genotypes (M_ε33)	82 (29 AD; 53 NCI)
Male *APOE* ε4 carriers (M_ε4x)	37 (27 AD; 10 NCI)
B. Number of nuclei per major cell class	
Cell class	**Number of nuclei**
Astrocytes (Ast)	99,034
CAMs	1516
Endothelial (End)	4756
Excitatory neurons (Exc)	700,456
Fibroblasts (Fib)	3180
Inhibitory neurons (Inh)	226,971
Microglia (Mic)	52,649
Oligodendrocytes (Oli)	447,617
OPC	61,883
Pericytes (Per)	3800
Smooth muscle cells (SMC)	1168
T cells	1740

categories. These include 14 excitatory neuron subtypes (Exc), 25 inhibitory neuron subtypes (Inh), one oligodendrocyte (Oli) subtype, one oligodendrocyte precursor cell (OPC) subtype, three astrocyte subtypes (Ast), and five immune cell types (microglia [Mic], central nervous system-associated macrophages [CAMs], and T cells). The dataset also encompasses several vascular cell types, including endothelial cells (End), smooth muscle cells (SMCs), fibroblasts (Fib), and pericytes (Per).

To confirm sex identity, we checked sex-linked gene expression and identified four samples with inconsistencies between the reported sex in the metadata and the expression patterns of sex-linked genes. As illustrated in Figure S1, Projid 50301963, which was annotated as female, exhibited no detectable *XIST* (female-specific) expression but high *UTY* (male-specific) expression across all major cell types. Similarly, Projid 11326252, 15114174, and 10277308, which were all labeled as male, showed strong *XIST* expression but no detectable *UTY*. Given the uncertainty regarding the true biological sex of these individuals and to avoid systematic misclassification bias in our sex-stratified analyses, we excluded these four samples from the present study, resulting in 214 female and 209 male donors.

For this study, we also excluded *APOE* ε2/ε4 samples ($n = 10$) due to the controversial nature of their association with disease risk. We also excluded samples lacking *APOE* genotype ($n = 2$) or *post mortem* interval (PMI) data ($n = 1$) and focused solely on NCI ($n = 142$) and AD ($n = 134$) samples (Table 1).

To investigate the impact of *APOE* genotypes, we grouped participants as follows: *APOE* ε2/ε2 and ε2/ε3 were categorized as *APOE* ε2 carriers (ε2x; $n = 38$), ε3/ε3 remained as ε3/ε3 ($n = 164$), and ε3/ε4 and ε4/ε4 were classified as *APOE* ε4 carriers (ε4x; $n = 74$) (Table 1). Among the 276 individuals included in these analyses, all but two were self-reported as White; the remaining two samples (one M_ε4x_NCI and one M_ε4x_AD) were reported as Black or African American.

2.2 | Cell-cluster-specific differential expression analysis

To investigate *APOE*-specific (ε2x, ε3/ε3, and ε4x) and sex-specific (F and M) transcriptional changes in AD, we performed cell-cluster-specific differential gene expression analysis across six combinatorial groups (F_ε2x, F_ε33, F_ε4x, M_ε2x, M_ε33, and M_ε4x). For each sex–*APOE* group, we compared samples from individuals with AD to control samples with NCI at the cell-cluster level to account for cell-type-specific transcriptional changes. We utilized the FindMarkers function in Seurat version 5 for cluster-specific DEG identification. Genes were included in the analysis if they were expressed in at least 10% of the cells in either group (min.pct = 0.1). To adjust for potential confounding factors, we incorporated covariates including nCount_RNA

(total RNA counts), PMI, and age at death. The only available technical covariate, sequencing batch, explained a negligible fraction of variance across genes and thus was not corrected. The Benjamini–Hochberg (BH) method was used to adjust *p* values for multiple testing.

Significant DEGs were defined as those meeting the following thresholds: adjusted *p*-value < 0.05 and absolute fold change (|FC|) > 1.3. Filtered genes that passed these criteria were included in downstream analyses. Enrichment analysis was performed by using R package GOtest (version 1.0.9) to test MSigDB canonical pathway gene sets (C2:CP). Enrichment significance was assessed using a hypergeometric test with BH correction for multiple testing with all genes in the dataset as the background. In this testing, pathways with adjusted *p* value < 0.05 were considered significant.

2.3 | Simulation-based power analysis

We conducted a power analysis using scDesign3,[31] a model-based framework for realistic single-cell RNA-seq (scRNA-seq) data simulation. Briefly, scDesign3 was first fit to the existing ROSMAP snRNA-seq microglia data to learn gene- and cell-type-specific expression distributions, mean–variance relationships, and zero inflation while accounting for experimental covariates. Using the fitted model, synthetic scRNA-seq datasets were generated under controlled study designs. In each simulation, predefined effect sizes (AD vs NCI fold changes) were introduced for a randomly selected subset of genes designated as truly differentially expressed, while all remaining genes were simulated with no differential expression. Differential expression analysis was then performed on the simulated datasets, and statistical power in each simulation was estimated as the proportion of truly differential genes detected at a false discovery rate (FDR) of 5% across repeated simulations. The final power estimate was defined as the mean statistical power across 100 simulations. This approach enabled systematic evaluation of statistical power as a function of effect size and sample size under realistic single-cell data characteristics.

2.4 | A novel metric for evaluating similarity of transcriptional patterns between sex or *APOE* genotype subgroups

To quantitatively evaluate the similarity of differential expression patterns across sexes and *APOE* genotypes for every gene, we developed and applied a novel similarity measure termed the Zhang-Yu similarity measure. This similarity measure calculates the similarity between two *N*-dimensional ternary vectors, say, ***X*** and ***Y***, representing differential expression statuses (AD vs NCI) of a given gene across differential expression contrasts of interest. In a ternary vector, each element takes one of three discrete values, −1, 0, and 1, representing significant downregulation, no significant change, and significant upregulation, respectively, from an AD versus NCI contrast. The similarity metric operates solely on directional states rather than continuous fold-change (FC) values. Because FC does not account for variability between the two groups being compared, FC alone is not sufficient to represent differential expression status. Instead, differential expression defined by both effect size (FC) and statistical significance provides a more accurate characterization of differences between groups. The similarity score between two ternary vectors ***X*** and ***Y*** is defined as

$$Score = \frac{(S_{1,1} + S_{-1,-1}) - 0.5 \times (S_{1,0} + S_{-1,0} + S_{0,1} + S_{0,-1}) - (S_{1,-1} + S_{-1,1})}{N}$$

where N denotes the number of differential expression tests and $S_{i,j}$ the number of occurrences of $X_k = i$ and $Y_k = j$, for $i, j \in (-1,\ 0,\ 1)$ and $k = 1,\ 2,\ \ldots,\ N$.

For each differential expression contrast, genes were encoded as a ternary state: +1 for significantly upregulated, −1 for significantly downregulated, and 0 for no significant change (based on adjusted *p* value and FC thresholds). The Zhang-Yu similarity measure operates exclusively on these directional states and does not incorporate continuous FC magnitudes.

In this framework, $S_{1,1}$ and $S_{-1,-1}$ represent concordant regulation in both groups (both upregulated or both downregulated), $S_{1,-1}$ and $S_{-1,1}$ represent opposite regulation between groups, and terms such as $S_{1,0}$ or $S_{-1,0}$ indicate regulation in one group but not the other. These components are weighted to quantify overall concordance or divergence across comparisons. Concordant directional changes increase similarity scores, whereas opposite directions of regulation reduce similarity.

While the established multi-condition differential expression analysis such as linear regression analysis is powerful in modeling marginal and interaction effects, it becomes challenging, less tractable, and harder to interpret when there are many factors or factor levels (such as the 54 cell types compounded by sex and *APOE* combinations) incorporated into the model. Certain parametric assumptions will be needed to fit the linear regression model for calling differential expressions. In the Zhang-Yu metric, we separate the differential expression analysis from the similarity score calculation and hence are flexible in choosing parametric or non-parametric models for differential expression analysis. Unlike the present Zhang-Yu metric that provides a similarity score ranging from −1 to 1, representing most divergent (lowest negative similarity scores) to most concordant transcriptional patterns (highest positive similarity scores) across groups, existing linear regression-based methods that basically test whether an effect size is different from 0 are limited in offering a comparable concordance ranking.

We applied this similarity measure to three key comparisons:

1. Female versus Male (i.e., sex difference):

   X: Discretized differential expression results from AD versus NCI within females across all cell clusters and *APOE* genotypes: F_ε2x_AD versus F_ε2x_NCI, F_ε33_AD versus F_ε33_NCI, and F_ε4x_AD versus F_ε4x_NCI.

   Y: Discretized differential expression results from AD versus NCI within males across all cell clusters and *APOE* genotypes: M_ε2x_AD versus M_ε2x_NCI, M_ε33_AD versus M_ε33_NCI, and M_ε4x_AD versus M_ε4x_NCI.

N: Total number of cell clusters (54) multiplied by three comparisons = 162.

2. *APOE* ε2x versus ε3/ε3:

   X: Discretized differential expression results from AD versus NCI within *APOE* ε2x across all cell clusters and sexes: F_ε2x_AD versus F_ε2x_NCI and M_ε2x_AD versus M_ε2x_NCI.

   Y: Discretized differential expression results from AD versus NCI within *APOE* ε3/ε3 across all cell clusters and sexes: F_ε33_AD versus F_ε33_NCI and M_ε33_AD versus M_ε33_NCI.

   N: Total number of cell clusters (54) multiplied by two sexes = 108.

3. *APOE* ε4x versus ε3/ε3:

   X: Discretized differential expression results from AD versus NCI within *APOE* ε4x across all cell clusters and sexes: F_ε4x_AD versus F_ε4x_NCI and M_ε4x_AD versus M_ε4x_NCI.

   Y: Discretized differential expression results from AD versus NCI within *APOE* ε3/ε3 across all cell clusters and sexes: F_ε33_AD versus F_ε33_NCI and M_ε33_AD versus M_ε33_NCI.

   N: Total number of cell clusters (54) multiplied by two sexes = 108.

Genes were then ranked based on their Zhang-Yu similarity scores. "Top" genes are those with the highest similarity scores, indicating the most concordant transcriptional patterns across the compared groups. "Bottom" genes are those with the lowest similarity scores, indicating the most divergent transcriptional patterns. These rankings depend solely on the directional consistency of differential expression and are independent of the magnitude of up- or down-regulation.

To evaluate significance for a Zhang-Yu similarity value for a given gene, we generated a null distribution by randomly shuffling the discretized differential expression states (−1, 0, +1) across all 54 cell types and six pairwise comparisons, thereby preserving the marginal distribution of states for each gene while removing the coordinated structure between female and male patterns. The Zhang-Yu similarity score was recalculated for each permuted dataset, and this procedure was repeated 10,000 times to obtain a gene-level null distribution of similarity scores. Using these null distributions, we estimated empirical FDR by comparing observed similarity scores to the permutation-derived null and the genome-wide distribution of observed scores. Applying an empirical FDR threshold of 0.05 identified 175 genes with significant similarity or divergence. Importantly, this set includes all the top 25 most similar genes from the real analysis and three of the bottom 25 most divergent genes, indicating that strong positive similarity is preferentially enriched, whereas only a small number of genes show statistically significant divergence.

2.5 | Validation of sex-specific genes in AD identified by Zhang-Yu similarity measure in an independent study of sex difference in AD

A previous study identified DEGs between AD and control in each sex group based on the RNA-seq data in the parahippocampal gyrus (PHG) in the Mount Sinai Brain Bank cohort.[27] Using the criteria of adjusted p value < 0.05 and |FC| > 1.2, there were 7001 and 1106 DEGs between female AD and female control and between male AD and male control, respectively. The much larger number of DEGs among the females was partially driven by the larger number of female AD and control samples in the dataset. To resolve the imbalanced power issue, we used a more stringent criterion of adjusted p value < 5E-4 and (FC > 1.2 or FC < 1/1.2) for the comparison of female AD versus female control and identified 1475 DEGs in female AD, which were closer to the 1102 DEGs in the male AD group. The two DEG signatures shared 230 genes, and 2117 DEGs were unique to either female AD or male AD. Among the 2117 sex-specific DEGs, 222 also showed sex difference detected by the Zhang-Yu ternary similarity measurement (Fisher's exact test $p = 0.18$, 1.06-fold enrichment).

We further applied an even more stringent criterion of adjusted p value < E-4 and (FC > 1.2 or FC < 1/1.2) for the comparison of female AD versus female control and identified 389 DEGs in the female AD group. The two DEG signatures shared 59 genes, and 1373 DEGs were unique to either female AD or male AD. Very interestingly, 161 of the 1373 sex-specific DEGs also showed sex difference detected by the Zhang-Yu ternary similarity measurement (Fisher's exact test $p = 0.00498$, 1.21-fold enrichment).

3 | RESULTS

3.1 | Cell-cluster-specific gene expression changes in AD in each sex–*APOE* subgroup

To investigate *APOE* (ε2x, ε3/ε3, and ε4x) and sex-specific (F and M) transcriptional changes in AD, we performed cell-cluster-specific differential gene expression analysis across six combinatorial groups (F_ε2x, F_ε33, F_ε4x, M_ε2x, M_ε33, and M_ε4x), excluding four samples with inconsistent metadata and sex-linked gene expression (Figure S1). For each group in each cell cluster, we compared gene expression profiles between AD and NCI participants. This stratification enabled us to resolve how *APOE* genotype and sex collectively influenced AD-associated molecular alterations across distinct cell clusters. As shown in Figures 1A,B and Table S1, Exc clusters exhibited a high number of DEGs in almost all sex–*APOE* groups. AD males carrying *APOE* ε2 (M_ε2x) had the most pronounced transcriptional response, with the highest DEG counts in Exc, Inh, OPC, and Mic clusters. This suggests a uniquely heightened transcriptional response to AD in these cell types within the M_ε2x subgroup.

Since some sex–*APOE* groups are less frequent than the others, there is an imbalanced sample size across sex–*APOE* combinations in the current cohort, e.g., the male *APOE* ε2 carrier group has only 13 samples while the female *APOE* ε2 carrier group has 25 samples. To investigate how the sample size difference might affect statistical power, we performed a simulation based empirical power analysis, focusing on the microglia (one of the least abundant major cell types in the brain) in the *APOE* ε2 carrier group (the least abundant *APOE* genotype group) across varying effect sizes (FCs). As illustrated in Figure

FIGURE 1 Cell-cluster-specific transcriptional signatures between AD and NCI across different sex–*APOE* subgroups. (A–B) Heatmaps showing number of up- (A; red) and downregulated (B; blue) differentially expressed genes (DEGs) between AD and NCI samples within each sex–*APOE* group (F_ε2x, F_ε33, F_ε4x, M_ε2x, M_ε33, M_ε4x) across all 54 cell clusters. Each row corresponds to a specific sex–*APOE* group, and each column represents a distinct cell cluster. DEGs were identified using MAST with Benjamini–Hochberg adjusted p value < 0.05 and $|FC| > 1.3$. (C–E) Comparative study of cell-cluster-specific transcriptional signatures between different sex–*APOE* subgroups. (C) Heatmap illustrating common, unique, and opposite DEGs between AD and NCI among female *APOE* groups (F_ε2x, F_ε33, and F_ε4x). From top to bottom, each panel corresponds to a pairwise comparison involving two *APOE* genotypes. (D) Heatmap illustrating common, unique, and opposite DEGs between AD and NCI among male *APOE* groups (M_ε2x, M_ε33, and M_ε4x). From top to bottom, each panel corresponds to a pairwise comparison involving two *APOE* genotypes as in (C). (E) Heatmap illustrating common, unique, and opposite DEGs for AD between males and females within each *APOE* genotype (ε2x, ε3/ε3, and ε4x). From top to bottom, each panel corresponds to a pairwise comparison between sexes for one *APOE* genotype.

S2, power increased monotonically with effect size (FC) in both sexes but was consistently higher in females than males, reflecting the larger number of female samples in the simulation (25 females vs 13 males). At small effect sizes (FC ≤1.2), power was negligible in both sexes. High power (≥80%) was achieved in females at FC ≥ 2.0, whereas males required larger effect sizes (FC ≥ 2.5) to reach comparable power. These results indicate that the study is well powered to detect large expression changes in both sexes but has limited power for small to moderate effects, particularly in males due to the smaller sample size.

3.2 | Comparison of transcriptional signatures across *APOE* genotypes in females and males

To determine whether *APOE* and sex interacted to shape molecular changes in AD across brain cell types, we first assessed the similarity of *APOE*-specific DEGs between males and females. For this, we first compared female AD-associated DEG signatures across *APOE* genotypes (F_ε2x, F_ε33, F_ε4x) using three pairwise contrasts (Figure 1C):

1. F_ε2x_AD versus F_ε2x_NCI and F_ε33_AD versus F_ε33_NCI
2. F_ε2x_AD versus F_ε2x_NCI and F_ε4x_AD versus F_ε4x_NCI
3. F_ε4x_AD versus F_ε4x_NCI and F_ε33_AD versus F_ε33_NCI

Notably, *APOE* ε4 carriers showed more distinct transcriptional changes compared to other genotypes, highlighting the impact of the ε4 genotype in females with AD.

The same analysis was applied to the male *APOE* groups (M_ε2x, M_ε33, and M_ε4x). As shown in Figure 1D, *APOE* ε2 carriers exhibited the most transcriptional divergence from other genotypes, particularly in Exc, Inh, and Ast clusters. This suggests that male *APOE* ε2 carriers may have more unique transcriptional programs than those observed in females.

3.3 | Comparison across sexes within each *APOE* genotype

We also examined the common and unique AD signatures between sexes for each *APOE* genotype. We compared *APOE*-specific DEGs of AD between females and males using the following pairwise contrasts (Figure 1E):

1. F_ε2x_AD versus F_ε2x_NCI and M_ε2x_AD versus M_ε2x_NCI
2. F_ε33_AD versus F_ε33_NCI and M_ε33_AD versus M_ε33_NCI
3. F_ε4x_AD versus F_ε4x_NCI and M_ε4x_AD versus M_ε4x_NCI

In contrast to *APOE* ε2 and *APOE* ε4 carriers, which exhibited more sex-specific transcriptional changes in AD, *APOE* ε3/ε3 groups had relatively fewer transcriptional differences between sexes across most cell clusters. This is consistent with the known biological role of the ε3/ε3 genotype, which is generally considered neutral in terms of AD risk, unlike the protective ε2 or risk-associated ε4 alleles. The limited sex-specific divergence in ε3/ε3 suggests a more stable transcriptional landscape, potentially reflecting the absence of strong disease-modifying pressures observed in ε2 or ε4 carriers.

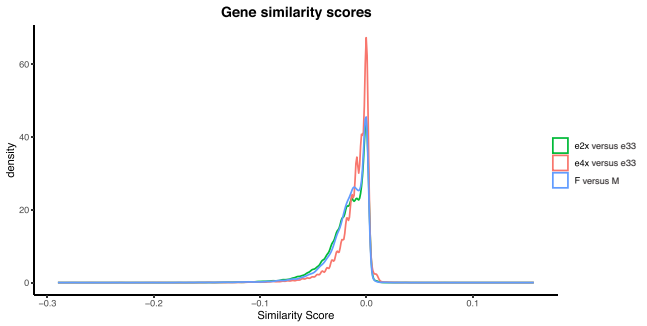

FIGURE 2 Distribution of gene similarity scores for different comparisons. Each curve represents similarity scores between groups across all clusters: blue – females versus males; green – *APOE* ε2x versus ε3/ε3; red – *APOE* ε4x versus ε3/ε3.

3.4 | Similarity measures reveal shared and distinct transcriptional changes across sexes and *APOE* genotypes in AD

For each gene profiled by snRNA-seq, we performed a series of cell-cluster-specific differential expression tests across sex and *APOE* genotype subgroups. We created and used the Zhang-Yu similarity measure to quantitatively compare gene expression patterns across sexes and *APOE* genotypes. With this approach, the differential expression status of a gene across multiple comparisons is represented by a ternary vector, with elements taking values of −1 for significant downregulation, 0 for no significant change, and +1 for significant upregulation. By contrasting ternary vectors between two conditions (e.g., females vs males), the Zhang-Yu similarity measure distinguishes the consistent changes from inconsistent changes, providing a quantitative measure of the directional consistency or divergence in gene expression changes. Positive scores indicate consistency, whereas negative scores reflect divergence.

We applied this similarity measure to compare transcriptional changes of AD versus NCI between females and males (i.e., sex difference), as well as between *APOE* ε2x and ε3/ε3, and between *APOE* ε4x and ε3/ε3 (Figure 2). While most genes had similarity scores close to zero, a greater number exhibited negative scores than positive scores (females vs males: 30.0% positive, 70.0% negative; *APOE* ε2x vs ε3/ε3: 35.1% positive, 64.9% negative; *APOE* ε4x vs ε3/ε3: 49.2% positive, 50.8% negative), indicating overall divergence in expression patterns. Using the procedure for estimating the significance of the Zhang-Yu similarity described in *Methods*, 293 and 2321 genes show significant similarity and difference in differential expression of AD versus control between males and females, respectively (Table S2). The 2321 genes with significant sex difference are enriched for the genes showing sex difference in differential expression between AD and control from the bulk tissue data in the PHG in the Mount Sinai Brain Bank cohort[27] with

hypergeometric test $p = 5E\text{-}3$ and 1.2-fold enrichment = 1.2 (Table S3) and the top three genes are *TMSB10* (similarity = −0.176, FDR = 0), *CLU* (similarity = −0.16, FDR = 0), *MALAT1* (similarity = −0.148, FDR = 0). The details of this independent validation can be found in the *Methods* section.

Figure 3A illustrates the top 25 genes with the highest similarity scores (most concordant) and bottom 25 genes with the lowest similarity scores (most divergent) for females versus males (sex difference). The heatmap depicts the frequency of all possible combinations of expression patterns between females and males, including consistent upregulation (1,1), consistent downregulation (−1,−1), and divergent or discordant patterns such as (1,0), (0,1), (1,−1), and (−1,1) (see *Methods*). As shown in the plot, genes with lower similarity scores are predominantly enriched for "opposite" and "different" expression cases, indicating divergent transcriptional responses between sexes. In contrast, genes with higher similarity scores tend to exhibit more "same" direction patterns, reflecting concordant transcriptional changes in both sexes. The validity of the similarity metric is further supported by the observation that several previously reported sex-specific AD genes, including *LINGO1* (similarity score: −0.275), *LINC00486* (similarity score: −0.216), and *CST3* (similarity score: −0.123), all exhibit negative similarity scores in our analysis.[32]

The four genes showing the most significant *APOE* genotype-dependent sex differences are *MT-ND2*, *SLC26A3*, *LINGO1*, and *RASGEF1B* (Table S2). These genes are more frequently upregulated in women with AD than in men with AD and more frequently downregulated in men with AD than in women with AD. A previous study showed that the top gene, *MT-ND2* (mitochondrially encoded NADH dehydrogenase 2), had increased mRNA expression in the blood of AD patients, but its function in AD brains has not been studied at all. *SLC26A3* and *RASGEF1B* have not been studied in AD or dementia at all. Downregulation of *LINGO1* (leucine-rich repeat neuronal protein) has been shown to improve cognitive performance of AD by reducing activated microglia,[33–35] but it is downregulated in 17 cell types and is not differentially expressed in cells of any other type in AD men with *APOE* ε2x carriers, suggesting a different role of *LINGO1* in AD men with *APOE* ε2x carriers.

The 25 genes with the most divergent similarity scores also include *CLU* (clusterin), a gene also known as Apolipoprotein J (*APOJ*) and which is associated with AD risk, inflammation, and modulation of Aβ clearance.[36–38] In addition, several heat shock proteins (HSPs), including *HSPB1*, *HSPB1A*, *HSPA1B*, and *HSPH1*, were also identified. All these HSPs are implicated in cellular stress responses and neurodegeneration.[39,40] These findings are interesting because *CLU* and HSPs both function as stress-induced chaperones and are involved in preventing protein aggregation induced by stress and maintaining cellular homeostasis.[41,42] Notably, the *CLU* promoter contains heat shock elements (HSEs), and its transcription is directly regulated by heterocomplexes formed by *HSF1* and *HSF2*, both of which are the primary and essential transcription factors that also govern classical HSP expression.[37,43] Their co-occurrence among the top sex-divergent genes suggests that the heat shock response pathway may be differentially regulated between sexes in AD, potentially contributing to sex-specific vulnerability and resilience to neurodegeneration.

Pathway enrichment analysis of the top 200 genes with the highest similarity scores and the bottom 200 genes with the lowest similarity scores further revealed distinct biological processes associated with shared and divergent transcriptional responses (Figure 3B). Immune-related and stress response pathways, including cellular responses to external stimuli, influenza infection, and nonsense-mediated decay, were enriched in the top 200 genes. Notably, these annotations largely reflect interferon/antiviral gene programs, which have been discussed as showing sex-dependent modulation in neurodegeneration and aging.[44] In contrast, the bottom 200 genes showed limited pathway enrichment, suggesting that conserved transcriptional responses across sexes may involve more heterogeneous or less pathway-convergent gene sets.

For the comparison between *APOE* ε2x and *APOE* ε3/ε3 genotypes, the top 25 genes (highest similarity scores when comparing *APOE* ε2x and ε3/ε3) and the bottom 25 genes (lowest similarity scores when comparing *APOE* ε2x and ε3/ε3) are shown in Figure 4A. The presence of *NEAT1* and *UBB* among low-similarity genes is consistent with previous observations in an AD mouse model showing elevated expression of these genes in *APOE* ε2 astrocytes.[45] The bottom 200 genes were enriched in pathways associated with translational regulation, such as cytoplasmic ribosomal proteins and eukaryotic translation elongation, as well as stress-response pathways like cellular responses to external stimuli. This pattern is strikingly similar to that observed in the 200 most sex-divergent genes (Figure 4B). This overlap likely reflects the disproportionately large number of DEGs in the male ε2x group, which contributes to both the sex and *APOE* ε2 genotype-associated transcriptional divergence. Meanwhile, the top 200 genes showed little to no enrichment, indicating that shared gene expression patterns between these genotypes were less functionally constrained to specific pathways.

For the comparison between *APOE* ε4x and *APOE* ε3/ε3 genotypes, the top 25 genes with the highest similarity scores when comparing *APOE* ε4x and ε3/ε3 and the bottom 25 genes with the lowest similarity scores when comparing *APOE* ε4x and ε3/ε3 are shown in Figure 5A. Among the bottom 25 genes, *HSPA1A*, *HSPA1B*, and *HSP90AA1* have been previously reported to be upregulated in brain End in *APOE* ε4 models, consistent with enhanced cellular stress responses.[46] The genes with the lowest similarity scores were enriched for the mitochondrial function and stress response pathways, including oxidative phosphorylation, electron transport chain, and cellular response to heat stress (Figure 5B). In contrast, the genes with the highest similarity scores were enriched in pathways such as the PDGFRB pathway, phosphatidylinositol (PI) metabolism, and the P53 regulation pathway.

3.5 | Sex-based divergence within *APOE* genotypes reveals genotype-specific transcriptional effects

To investigate sex-specific transcriptional responses across *APOE* genotypes, we compared gene expression changes between females

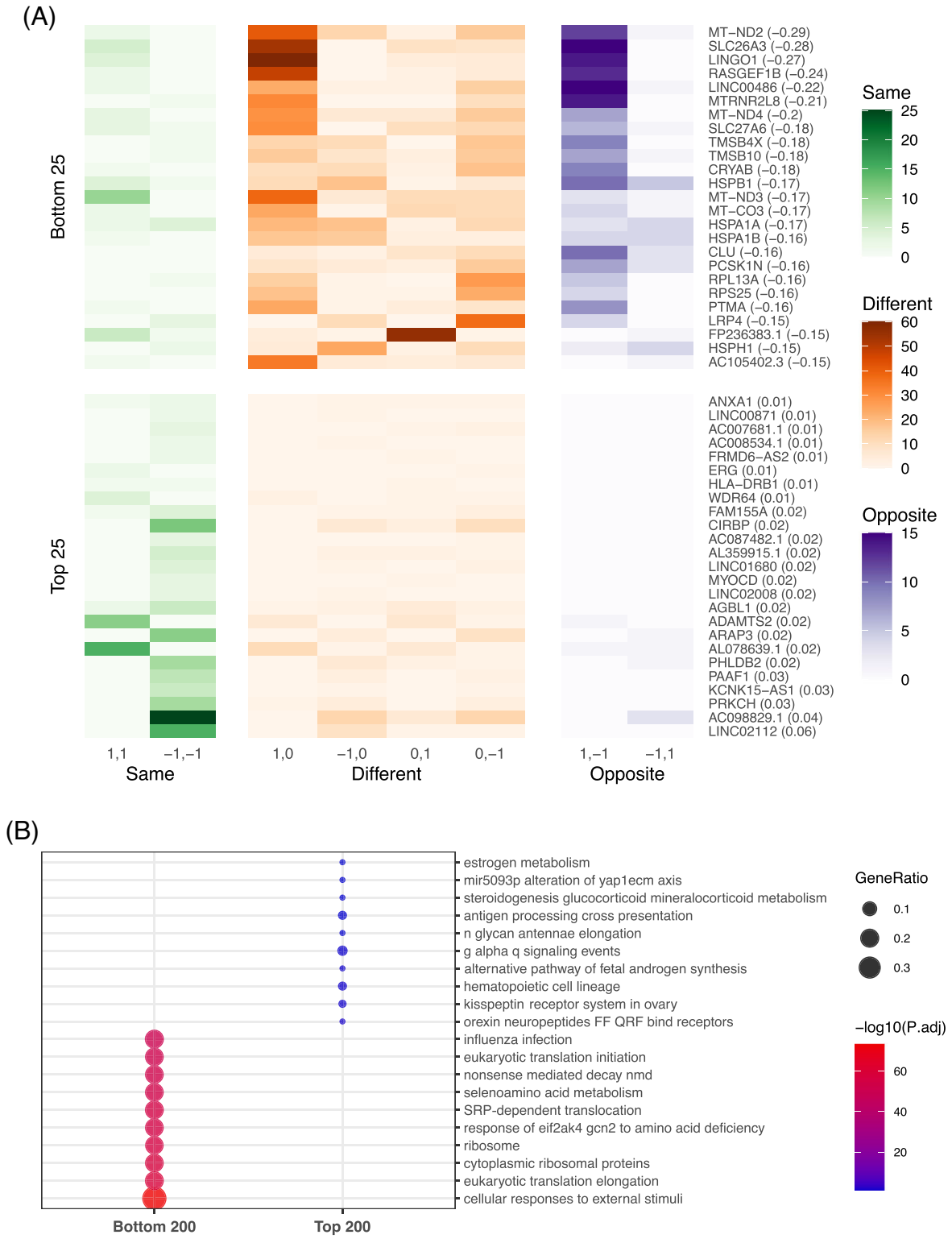

FIGURE 3 Sex-specific and shared transcriptional responses in AD. (A) Heatmap of top 25 and bottom 25 genes ranked by similarity scores, with top genes showing the highest concordance and bottom genes showing the greatest divergence. Color intensity indicates the number of occurrences with expression changes that are the same, different, or opposite between females and males. Discrete values –1, 0, and 1 indicate downregulation, no significant change, and upregulation, respectively. (B) Dotplot of MSigDB canonical pathways (C2:CP) enriched in top 200 and bottom 200 genes ranked by similarity scores (Benjamini–Hochberg adjusted p value < 0.05).

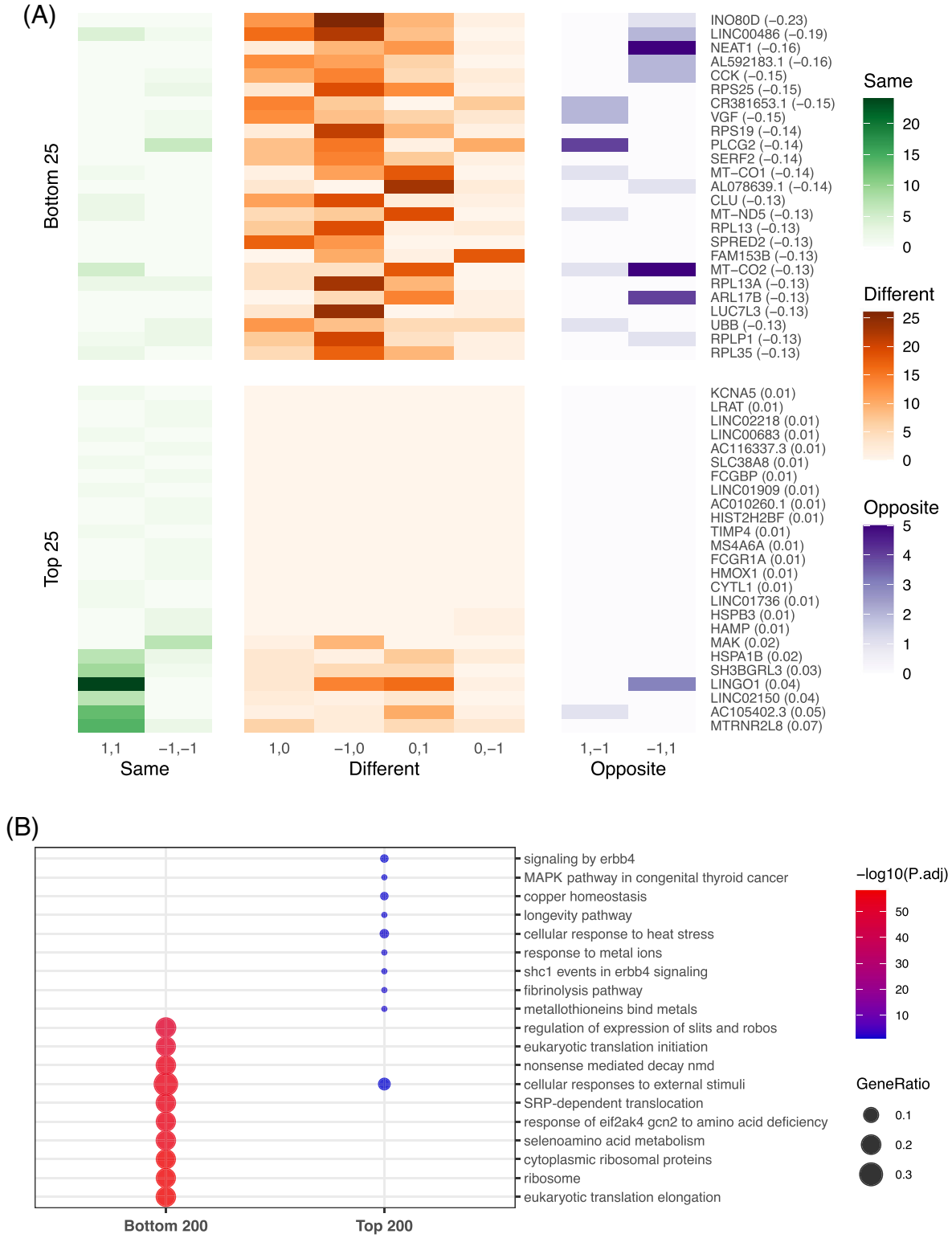

FIGURE 4 *APOE ε2*-specific and shared transcriptional responses in AD. (A) Heatmap of top 25 and bottom 25 genes ranked by similarity scores, with the top genes showing the highest concordance and the bottom genes showing the greatest divergence. Color intensity is defined as in Figure 3B. (B) Dotplot of MSigDB canonical pathways (C2:CP) enriched in the top 200 and bottom 200 genes ranked by similarity scores (Benjamini–Hochberg adjusted p value < 0.05).

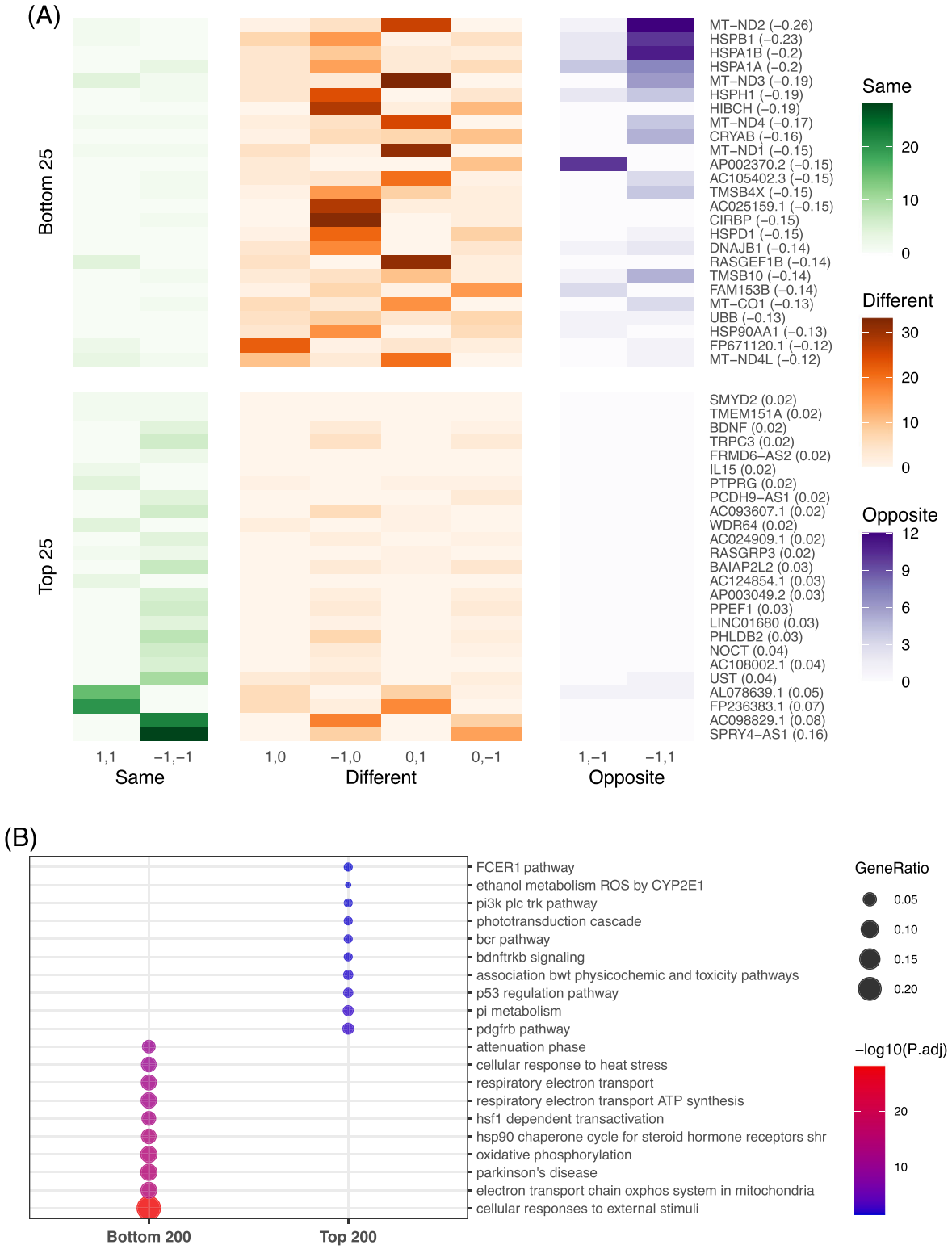

FIGURE 5 *APOE ε4*-specific and shared transcriptional responses in AD. (A) Heatmap of the top 25 and bottom 25 genes by similarity scores, with top genes showing the highest concordance and bottom genes showing the greatest divergence. Color intensity is defined as in Figure 3B. (B) Dotplot of the MSigDB canonical pathways (C2:CP) enriched in the top 200 and bottom 200 genes ranked by similarity scores (Benjamini–Hochberg adjusted p value < 0.05).

and males within each *APOE* genotype group using the Zhang-Yu similarity measure. This analysis reveals sex–*APOE* interaction effects, showing how sex influences AD-related transcriptional changes differently across *APOE* genotypes. Figures 6A presents the top 10 genes and the bottom 10 genes for each comparison. To further explore the biological relevance of genes showing sex differences, we performed pathway enrichment analysis on the bottom 200 genes from each comparison (Figure 6B). In *APOE* ε2x and *APOE* ε3/ε3 groups, sex-biased genes were predominantly enriched in ribosome- and translation-related pathways. Across all three *APOE* genotypes, sex-specific divergent genes converged on molecular chaperone processes, including the HSP90 cycle for steroid receptors and the HSF1 heat shock response, with the strongest enrichment observed in *APOE* ε4 carriers. Pathways linked to infectious disease, nervous system development, and cellular responses to external stimuli were also consistently enriched across *APOE* genotypes. Notably, immune-related enrichments displayed genotype-specific patterns: The innate immune system was enriched in *APOE* ε2 and *APOE* ε4 carriers; interleukin signaling was enriched in *APOE* ε2 carriers and *APOE* ε3/ε3 samples; and cytokine signaling in the immune system was uniquely enriched in *APOE* ε3/ε3 samples. These patterns reveal a clear interplay between sex and *APOE* genotype in shaping AD-associated transcriptional programs, pinpointing distinct molecular pathways through which this interaction may influence disease pathogenesis.

3.6 | *CLU* exhibits *APOE*- and sex-dependent transcriptional changes across cell types

Among the genes showing strong sex- and *APOE*-specific divergence, *CLU* (clusterin) stood out due to its contrasting expression patterns across astrocyte and excitatory neuron subclusters (Figure 7). In astrocyte subclusters, *CLU* was upregulated in F_ε2x but downregulated in M_ε2x. In excitatory neurons, *CLU* exhibited a more complex pattern: It was upregulated in F_ε2x and M_ε4x but downregulated in F_ε4x and M_ε2x, indicating an inversion of expression direction across sexes within both protective and risk-associated genotypes. These findings highlight *CLU* as a key gene exhibiting sex–*APOE* interaction effects, possibly reflecting *CLU*'s known roles in lipid metabolism, neuroinflammation, and amyloid clearance.

4 | DISCUSSION

This study presents a comprehensive analysis of sex- and *APOE*-specific transcriptional changes in AD using a large snRNA-seq dataset from the ROSMAP cohort. By performing differential gene expression analysis across six stratified sex–*APOE* groups and applying a novel similarity metric, the Zhang-Yu similarity measure, we uncovered shared and divergent transcriptional patterns across sexes and *APOE* genotypes. These analyses revealed several key biological themes, including sex- and *APOE*-dependent regulation of *CLU* and heat shock proteins, *APOE* genotype-specific translational and mitochondrial pathways, and distinct immune signaling signatures. These findings highlight the interplay between genetic risk, sex, and cell-type-specific transcriptional responses in AD pathophysiology.

Male *APOE* ε2 carriers had most DEGs when comparing AD to NCI samples, suggesting a heightened transcriptional response in this subgroup. A majority of AD signatures were identified in excitatory neurons, inhibitory neurons, astrocytes, OPCs, and one specific microglia cluster, highlighting the importance of these cell types in transcriptional responses to AD across all sex–*APOE* groups. Conversely, several cell clusters, including End, CAMs, Per, SMCs, and T cells, showed no significant transcriptional changes, indicating a limited or negligible response to AD-related pathology in these populations, in part due to the small number of cells available.

In the comparison of transcriptional signatures across *APOE* genotypes in females, F_ε4x AD signatures were notably divergent from those of F_ε2x and F_ε33. This divergence was particularly evident in comparisons such as F_ε2x_AD versus F_ε2x_NCI and F_ε4x_AD versus F_ε4x_NCI, and F_ε4x_AD versus F_ε4x_NCI and F_ε33_AD versus F_ε33_NCI. Both comparisons displayed a higher number of DEGs that were unique to one condition. These unique DEGs suggest distinct transcriptional responses in F_ε4x carriers, consistent with the known heightened AD risk associated with *APOE* ε4. Similarly, in males, M_ε2x_AD signatures were significantly divergent from M_ε4x and M_ε33_AD signatures. These findings highlight the distinct transcriptional responses associated with *APOE* ε4 in females and *APOE* ε2 in males, reflecting genotype-specific roles in AD pathology.

The use of the Zhang-Yu similarity measure allowed us to quantify shared and divergent transcriptional patterns across a large number of differential expression tests, such as the 54 cell clusters paired by sex or *APOE* genotype in this study. Genes with positive similarity scores represented conserved transcriptional responses, reflecting core molecular processes shared across sexes and genotypes. Conversely, genes with negative similarity scores highlighted subgroup-specific pathways, particularly in immune responses and stress-related mechanisms. These patterns reinforce the complexity of AD pathology and emphasize the importance of examining both shared and divergent molecular changes in understanding the disease. While this approach effectively identifies genes that change either consistently or distinctively across multiple conditions (i.e., cell clusters paired by sex or *APOE* genotype), its limitation lies in its reduced sensitivity to detect genes exhibiting changes restricted to only a few or unique conditions (e.g., cell types). As this similarity measure depends on differential expression status across various comparisons of interest, the selection of thresholds for FC and FDR is critical. We suggest using the thresholds that are widely accepted in the field.

We extended this analysis by comparing transcriptional changes in AD versus NCI between females and males within each *APOE* genotype, revealing *APOE* genotype-specific sex effects on AD-related transcriptional responses. Among *APOE* ε2 carriers, divergent genes were uniquely enriched in innate immune and antiviral pathways, including influenza infection and innate immune system. In contrast, *APOE* ε4 carriers showed pronounced sex-specific divergence in stress-related and neurodevelopmental pathways, including HSP90 chaperone cycle, reg-

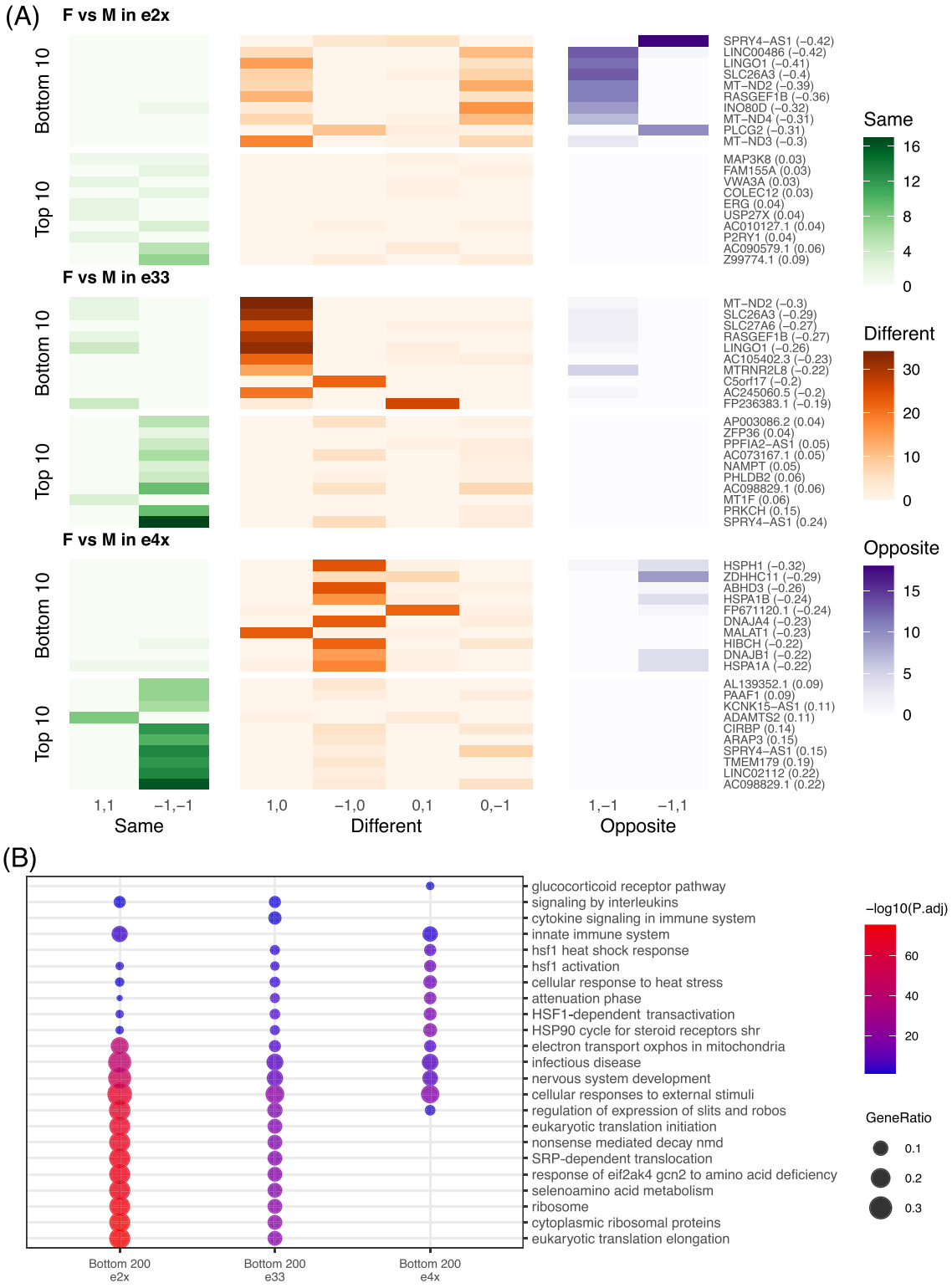

FIGURE 6 Genes displaying consistent or divergent expression changes between females and males within each *APOE* genotype group. (A) From top to bottom, heatmaps show both the top 10 and bottom 10 genes by sex divergence similarity scores identified in *APOE* ε2 carriers, *APOE* ε3 homozygotes, and *APOE* ε4 carriers, respectively. Color intensity is defined as in Figure 3B. (B) Enrichment of MSigDB canonical pathways (C2:CP) among the top 200 genes with the greatest sex differences within each *APOE* genotype group (Benjamini–Hochberg adjusted *p* value < 0.05).

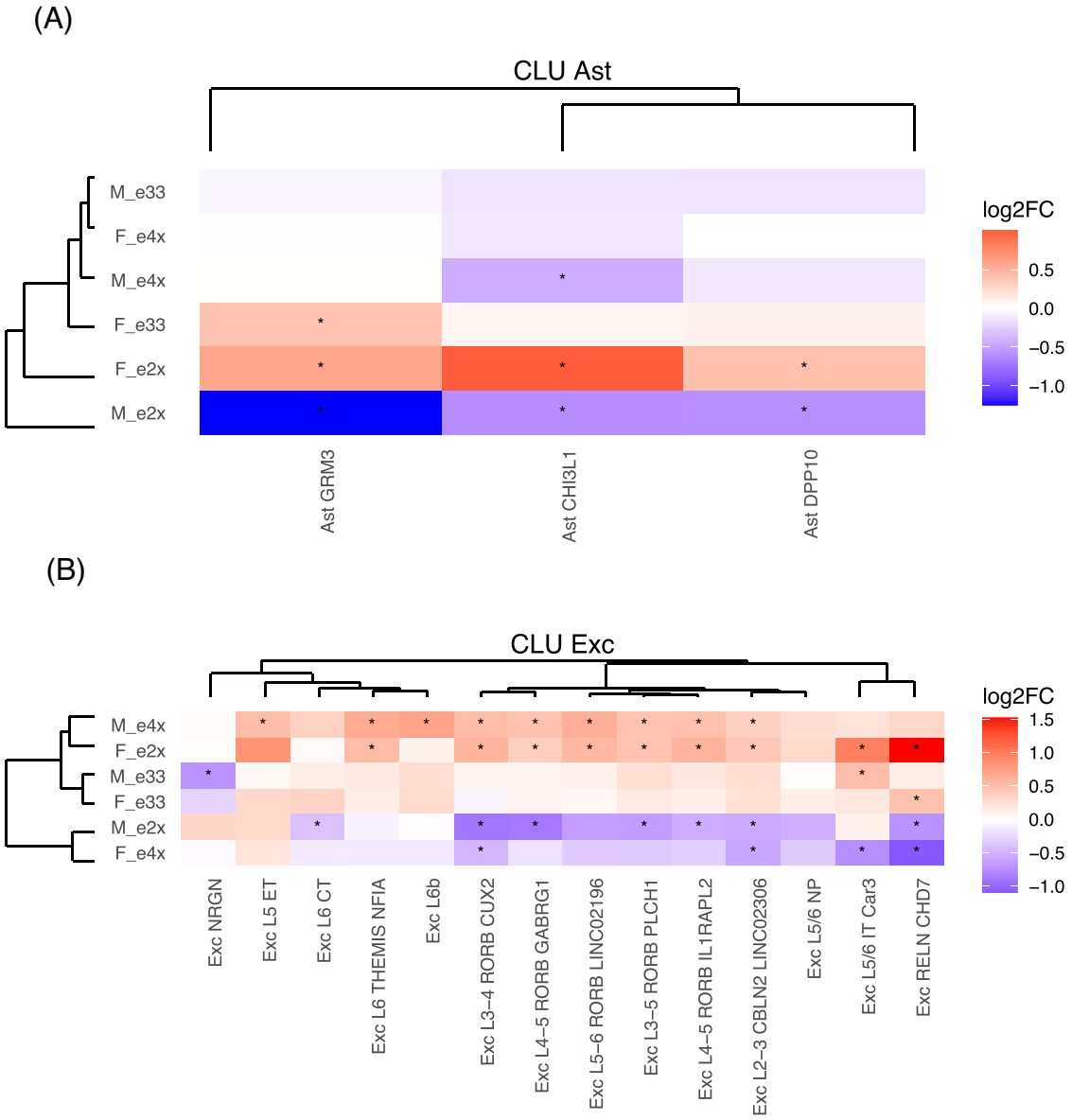

FIGURE 7 Cluster-specific *CLU* expression changes across sex–*APOE* subgroups. (A) Heatmap showing log2 fold changes of *CLU* expression in astrocytes (A) and excitatory neuron (B) subclusters. Asterisks (*) indicate significant differential expression identified using MAST, with Benjamini–Hochberg adjusted p value < 0.05.

ulation of HSF1-mediated heat shock response, infectious disease, and nervous system development.

Interestingly, we identified *CLU* as an example of sex- and *APOE*-dependent expression changes. *CLU* was downregulated in M_ε2x and F_ε4x but upregulated in F_ε2x and M_ε4x within excitatory neurons and also displayed a sex-divergent pattern in astrocytes, being upregulated in F_ε2x and downregulated in M_ε2x. These findings suggest that *CLU* expression is stratified by an interaction between sex and *APOE* genotype, which may reflect its multifaceted role in amyloid clearance, inflammation, and lipid metabolism.

It should also be noted that hormone-like estradiol fluctuation may modulate *APOE* expression in a genotype-specific manner. The application of the proposed Zhang-Yu similarity metric revealed that some key hormone-related and sex-linked genes exhibit sex-specific dysregulation in AD. The 2321 genes that show significant *APOE* genotype-dependent difference between males and females include one hormone gene (*CYP1B1*) and 91 sex-linked genes (Tables S4 and S5). The top sex-linked gene showing the largest sex difference is *TMSB4X* (Table S6). A recent study showed that the expression level of the gene *TMSB4X* decreased both in FAD organoids' neurons and AD patients' excitatory neurons.[47] Our analysis shows that *TMSB4X* is indeed downregulated in inhibitory and excitatory neurons in AD males carrying any *APOE* genotype and in AD females carrying only APOE ε4 but is upregulated in AD females carrying *APOE* ε2 and *APOE* ε3/ε3 alleles. On the other hand, a recent genome-wide association study of cortical tau identified the CYP1B1-RMDN2 locus associated with tau deposition.[47] Our data show that *CYP1B1* is upregulated in the *CBLN2*- and *LINC02306*-positive excitatory neurons in

AD females carrying *APOE* ε2 alleles but downregulated in *RORB*- and *CUX2*-positive excitatory neurons in AD females carrying *APOE* ε3/ε3 alleles. However, *CYP1B1* shows no significant changes in other comparisons involving AD females or in any comparison between AD males and control males. Therefore, our system-level analysis reveals a more comprehensive and granular atlas of brain cell-type-specific, *APOE* genotype-dependent sex differences in gene expression changes in AD. The differential lipid-binding capacity of *APOE* isoforms may also interact with sex-specific lipidomic profiles. Further studies are needed to investigate how sex hormones, X-chromosome dosage, or *APOE* protein isoforms might mechanistically drive the observed sex- and *APOE*-specific transcriptional patterns in AD.

Several limitations of this study should be acknowledged. First, detailed medication history data could not be incorporated as covariates since the public ROSMAP data, as accessed through the AMP-AD Knowledge Portal, did not include patient medication history data. Medication use, particularly for drug classes related to hormone replacement therapy, cardiovascular disease, neuropsychiatric symptoms, and inflammation, may differ systematically by sex and may also interact with *APOE* genotype. As a result, some of the observed sex–*APOE* associated transcriptional differences, especially within immune and metabolic pathways, may partially reflect medication related effects rather than disease biology alone. Second, the present study is computational in nature and does not include direct functional validation of the identified genes and pathways. While the observed sex–*APOE*-dependent transcriptional signatures generate testable hypotheses, experimental validation will be needed to establish any causal mechanisms. Future studies will be critical such as (1) additional high-level network biology approaches applied to identify causal drivers of observed key transcriptional changes that are specific to each sex–*APOE* group or shared across groups and (2) functional characterization of key findings in vitro and/or in vivo using brain cells and co-cultures derived from human-induced pluripotent stem cells (hiPSCs) of male and female AD and control patients with different *APOE* genotypes and relevant mouse models, as we did previously.[48–53] It would be important to investigate the translational relevance of observed sex- and *APOE*-dependent regulation of *CLU*, mitochondria functions, heat shock response pathways, and immune signaling programs in AD. Third, this study has reduced power to detect small to moderate expression changes in rare cell populations, particularly within under-represented genotype–sex strata. Power differences between sample groups are largely driven by sample size imbalance rather than biological effects, limiting sensitivity in small groups, e.g., male *APOE* ε2 carriers. Consequently, null results in these settings should be interpreted with caution, as modest but biologically relevant effects may remain undetected. Furthermore, we did not analyze the MCI cases given the heterogeneity of this group. However, it would be a great follow-up study to determine the temporal dynamics of observed sex- and *APOE*-dependent transcriptional changes during disease progression. Fourth, there is a lack of racial and ancestral diversity in the study cohort, which in this case was predominantly composed of self-identified white individuals. This is particularly problematic for AD research because the frequency and risk impact of *APOE* gene variants differ significantly across populations.[54–56] For example, *APOE* ε4 risk allele is far more common in some populations but confers a different magnitude of AD risk depending on an individual's genetic ancestry. Consequently, the links between sex, *APOE*, and gene expression patterns identified in this study may be specific to the study's population and may not generalize to others. Therefore, this limitation underscores a critical need to validate results in ancestrally diverse cohorts.

Overall, this study highlights the intricate interplay between sex and *APOE* genotype in shaping transcriptional responses in AD. By integrating cell-cluster-specific analyses with a novel similarity scoring approach, we provide a detailed view of the molecular heterogeneity underlying AD. Our findings emphasize the importance of accounting for both sex and genetic context when interpreting disease-associated transcriptional changes. These findings pave the way for future research to further elucidate the functional implications of identified pathways and develop precision medicine strategies that address the diverse molecular profiles of AD patients.

ACKNOWLEDGMENTS

The ROSMAP datasets are available via the AD Knowledge Portal (https://adknowledgeportal.org). The AD Knowledge Portal is a platform for accessing data, analyses, and tools generated by the Accelerating Medicines Partnership (AMP-AD) Target Discovery Program and other National Institute on Aging (NIA)-supported programs to enable open-science practices and accelerate translational learning. We thank all the participants of the ROSMAP study for their participation and generous donation of brains. This work was supported in part by funding from the National Institutes of Health (NIH) RF1 (RF1AG054014), R56 (R56AG058655), and RF1 (RF1AG074010) to DC and BZ, NIH U01 (UO1AG046170), RF1 (RF1AG057440), RO1(RO1AG057907) to BZ, and NIH R21AG077168, NIH RF1AG077828, Alzheimer's Association AARG-22-928419 to MW. This work was also supported in part through the computational and data resources and staff expertise provided by Scientific Computing and Data at the Icahn School of Medicine at Mount Sinai and supported by Clinical and Translational Science Awards (CTSA) grant UL1TR004419 from the National Center for Advancing Translational Sciences. Research reported in this publication was also supported by the Office of Research Infrastructure of the NIH under the award numbers S10OD026880 and S10OD030463. The content is solely the responsibility of the authors and does not necessarily represent the official views of the NIH. These funding sources had no role in the design and conduct of the study or collection, management, and analysis of the data.

CONFLICT OF INTEREST STATEMENT

The authors declare no conflicts of interest. Author disclosures are available in the Supporting Information.

CONSENT STATEMENT

Informed consent was obtained from each subject, and the Religious Orders Study and Rush Memory and Aging Project were each approved by an Institutional Review Board of Rush University Medical Center.

Participants also signed an Anatomic Gift Act and a repository consent to allow their data to be repurposed. Details of the clinical and pathological data collection methods were previously reported.

ORCID

Minghui Wang https://orcid.org/0000-0001-9171-4962

REFERENCES

1. Karantzoulis S, Galvin JE. Distinguishing Alzheimer's disease from other major forms of dementia. *Expert Rev Neurother*. 2011;11:1579-1591. doi:10.1586/ern.11.155
2. 2020 Alzheimer's disease facts and figures. *Alzheimers Dement*. 2020;16:391-460. doi:10.1002/alz.12068
3. Barnes LL, Wilson RS, Schneider JA, Bienias JL, Evans DA, Bennett DA. Gender, cognitive decline, and risk of AD in older persons. *Neurology*. 2003;60:1777-1781. doi:10.1212/01.wnl.0000065892.67099.2a
4. Edland, SD, Rocca, WA, Petersen, RC, Cha, RH, Kokmen, E Dementia and Alzheimer disease incidence rates do not vary by sex in Rochester, Minn. *Arch Neurol*. 2002;59:1589-1593. doi:10.1001/archneur.59.10.1589
5. Kawas, C, Gray, S, Brookmeyer, R, Fozard, J, Zonderman, A Age-specific incidence rates of Alzheimer's disease: the Baltimore Longitudinal Study of Aging. *Neurology*. 2000;54:2072-2077. doi:10.1212/wnl.54.11.2072
6. Plassman BL, Langa KM, McCammon RJ, et al. Incidence of dementia and cognitive impairment, not dementia in the United States. *Ann Neurol*. 2011;70: 418-426. doi:10.1002/ana.22362
7. Seshadri S, Wolf PA, Beiser A, et al. Lifetime risk of dementia and Alzheimer's disease. The impact of mortality on risk estimates in the Framingham study. *Neurology*. 1997;49:1498-1504. doi:10.1212/wnl.49.6.1498
8. Hua X, Hibar DP, Lee S, et al. Sex and age differences in atrophic rates: an ADNI study with n = 1368 MRI scans. *Neurobiol Aging*. 2010;31:1463-1480. doi:10.1016/j.neurobiolaging.2010.04.033
9. Skup M, Zhu H, Wang Y, Giovanello KS, et al. Sex differences in grey matter atrophy patterns among AD and aMCI patients: results from ADNI. *Neuroimage*. 2010;56:890-906. doi:10.1016/j.neuroimage.2011.02.060
10. Ardekani, BA, Convit, A, Bachman, AH Analysis of the MIRIAD data shows sex differences in hippocampal atrophy progression. *J Alzheimers Dis*. 2016;50:847-857. doi:10.3233/JAD-150780
11. Mayeux, R Epidemiology of neurodegeneration. *Annu Rev Neurosci*. 2003;26: 81-104.
12. Farrer, LA Effects of age, sex, and ethnicity on the association between apolipoprotein E genotype and Alzheimer disease. A meta-analysis. APOE and Alzheimer disease meta analysis consortium. *JAMA*. 1997;278: 1349-1356.
13. Neu SC, Pa J, Kukull W, Beekly D et al. Apolipoprotein E genotype and sex risk factors for Alzheimer disease: a meta-analysis. *JAMA Neurol*. 2017;74: 1178-1189. doi:10.1001/jamaneurol.2017.2188
14. Yan S, Zheng C, Paranjpe MD, Li J, Benzinger TLS, Lu J, Zhou Y Association of sex and APOE ε4 with brain tau deposition and atrophy in older adults with Alzheimer's disease. *Theranostics*. 2020;10: 10563-10572. doi:10.7150/thno.48522
15. Altmann, A, Tian, L, Henderson, VW, Greicius, MD, Alzheimer's Disease Neuroimaging Initiative Investigators. Sex modifies the APOE-related risk of developing Alzheimer disease. *Ann Neurol*. 2014;75(4):563-573. doi:10.1002/ana.24135
16. Hohman TJ, Dumitrescu L, et al. Sex-specific association of apolipoprotein E with cerebrospinal fluid levels of tau. *JAMA Neurol*. 2018;75, 989-998. doi:10.1001/jamaneurol.2018.0821
17. Cavedo E, Chiesa PA, Houot M, et al. Sex differences in functional and molecular neuroimaging biomarkers of Alzheimer's disease in cognitively normal older adults with subjective memory complaints. *Alzheimer's Dement*. 2018;14:1204-1215. doi:10.1016/j.jalz.2018.05.014
18. Sampedro F, Vilaplana E, et al. APOE-by-sex interactions on brain structure and metabolism in healthy elderly controls. *Oncotarget*. 2015;6(29):26663-26674. doi:10.18632/oncotarget.5185
19. Sundermann EE, Tran M, Maki PM, Bondi MW. Sex differences in the association between apolipoprotein E epsilon4 allele and Alzheimer's disease markers. *Alzheimer's Dement (AMST)*. 2018;10:438-447. doi:10.1016/j.dadm.2018.06.004
20. Kim J, Fischer CE, Schweizer TA, Munoz DG. Gender and pathology-specific effect of apolipoprotein E genotype on psychosis in Alzheimer's disease. *Curr Alzheimer Res*. 2017;14:834-840. doi:10.2174/1567205014666170220150021
21. Xing Y, Qin W, Li F, Jia XF, Jia J. Apolipoprotein E epsilon4 status modifies the effects of sex hormones on neuropsychiatric symptoms of Alzheimer's disease. *Dement Geriatr Cogn Disord*. 2012;33:35-42. doi:10.1159/000336600
22. Shinohara M, Murray ME, Frank RD, Shinohara M, et al. Impact of sex and APOE4 on cerebral amyloid angiopathy in Alzheimer's disease. *Acta Neuropathol*. 2016;132:225-234. doi:10.1007/s00401-016-1580-y
23. Hsu, M, Dedhia, M, Crusio, WE, Delprato, A. Sex differences in gene expression patterns associated with the APOE4 allele. *F1000Research*. 2019;8:387. doi:10.12688/f1000research.18671.2
24. Moser VA, Workman MJ, Hurwitz SJ, Lipman RM, Pike CJ, Svendsen CN. Microglial transcription profiles in mouse and human are driven by APOE4 and sex. 2021. *iScience*. 24:103238. doi:10.1016/j.isci.2021.103238
25. Paranjpe MD, Belonwu S, Wang JK, Oskotsky T, et al. Sex-specific cross tissue meta-analysis identifies immune dysregulation in women with Alzheimer's disease. *Front Aging Neurosci*. 2021;13, 735611. doi:10.3389/fnagi.2021.735611
26. Arnold M, Nho K, Kueider-Paisley A, Massaro T, et al. Sex and APOE epsilon4 genotype modify the Alzheimer's disease serum metabolome. *Nat Commun*. 2020;11:1148. doi:10.1038/s41467-020-14959-w
27. Guo L, Cao J, Hou J, Li Y, et al. Sex specific molecular networks and key drivers of Alzheimer's disease. *Molecular neurodegeneration* 2023;18:39. doi:10.1186/s13024-023-00624-5
28. Wang M, Roussos P, McKenzie A, Zhou X, et al. Integrative network analysis of nineteen brain regions identifies molecular signatures and networks underlying selective regional vulnerability to Alzheimer's disease. *Genome Medicine*. 2016;8:104. doi:10.1186/s13073-016-0355-3
29. De Jager PL, Ma Y, McCabe C, Xu J, et al. A multi-omic atlas of the human frontal cortex for aging and Alzheimer's disease research. *Sci Data*. 2018;5:180142. doi:10.1038/sdata.2018.142
30. Mathys H, Peng Z, Boix CA, Victor MB, et al. Single-cell atlas reveals correlates of high cognitive function, dementia, and resilience to Alzheimer's disease pathology. *Cell*. 2023;186, 4365-4385 e4327. doi:10.1016/j.cell.2023.08.039
31. Song D, Wang Q, Yan G, Liu T, Sun T, Li JJ scDesign3 generates realistic in silico data for multimodal single-cell and spatial omics. *Nat Biotechnol*. 2024;42:247-252. doi:10.1038/s41587-023-01772-1
32. Belonwu SA, Li Y, Bunis D, Rao AA, et al. Sex-stratified single-cell RNA-Seq analysis identifies sex-specific and cell type-specific transcriptional responses in Alzheimer's disease across two brain regions. *Mol Neurobiol*. 2022;59:276-293. doi:10.1007/s12035-021-02591-8
33. Castanho I, Naderi Yeganeh P, Boix CA, et al. Molecular hallmarks of excitatory and inhibitory neuronal resilience to Alzheimer's disease. *Mol Neurodegener*. 2025;20:103. doi:10.1186/s13024-025-00892-3
34. He Qi, Jiang L, Zhang Yi, et al. Anti-LINGO-1 antibody ameliorates cognitive impairment, promotes adult hippocampal neurogenesis, and increases the abundance of CB1R-rich CCK-GABAergic interneurons

in AD mice. *Neurobiol Dis*. 2021;156:105406. doi:10.1016/j.nbd.2021.105406g
35. Xie Yu-H, Jiang L, Zhang Yi, et al. Antagonizing LINGO-1 reduces activated microglia and alleviates dendritic spine loss in the hippocampus of APP/PS1 transgenic mice. *Neurosci Lett*. 2024;820:137612. doi:10.1016/j.neulet.2023.137612
36. Andrews SJ, Renton AE, Fulton-Howard B, Podlesny-Drabiniok A, Marcora E, Goate AM. The complex genetic architecture of Alzheimer's disease: novel insights and future directions. *EBioMedicine*. 2023;90:104511. doi:10.1016/j.ebiom.2023.104511
37. Nuutinen T, Suuronen T, Kauppinen A, Salminen A Clusterin: a forgotten player in Alzheimer's disease. *Brain Res Rev*. 2009;61:89-104. doi:10.1016/j.brainresrev.2009.05.007
38. Villegas-Llerena C, Phillips A, Garcia-Reitboeck P, Hardy J, Pocock JM. Microglial genes regulating neuroinflammation in the progression of Alzheimer's disease. *Curr Opin Neurobiol*. 2016;36:74-81. doi:10.1016/j.conb.2015.10.004
39. Paul, S, Mahanta, S Association of heat-shock proteins in various neurodegenerative disorders: is it a master key to open the therapeutic door?. *Mol Cell Biochem*. 2014;386:45-61. doi:10.1007/s11010-013-1844-y
40. Yenari, MA, Giffard, RG, Sapolsky, RM, Steinberg, GK The neuroprotective potential of heat shock protein 70 (HSP70). *Mol Med Today*. 1999;5:525-531. doi:10.1016/s1357-4310(99)01599-3
41. Lee J, Hong S-W, Kwon H, Park SeE, et al. Resveratrol, an activator of SIRT1, improves ER stress by increasing clusterin expression in HepG2 cells. *Cell Stress Chaperones*. 2019;24:825-833. doi:10.1007/s12192-019-01012-z
42. Foster, EM, Dangla-Valls, A, Lovestone, S, Ribe, EM & Buckley, NJ Clusterin in Alzheimer's disease: mechanisms, genetics, and lessons from other pathologies. *Front Neurosci*. 2019;13:164. doi:10.3389/fnins.2019.00164
43. Vihervaara A, Mahat DB, Himanen SV, Blom MAH, Lis JT, Sistonen L Stress-induced transcriptional memory accelerates promoter-proximal pause release and decelerates termination over mitotic divisions. *Mol Cell*. 2021;81:1715-1731 e1716. doi:10.1016/j.molcel.2021.03.007
44. Sirkis DW, Oddi AP, Jonson C, Bonham LW, Hoang PT, Yokoyama JS The role of interferon signaling in neurodegeneration and neuropsychiatric disorders. *Frontiers in Psychiatry*. 2024;15:1480438. doi:10.3389/fpsyt.2024.1480438
45. Preman P, Moechars D, Fertan E et al. APOE from astrocytes restores Alzheimer's abeta-pathology and DAM-like responses in APOE deficient microglia. *EMBO Mol Med*. 2024;16:3113-3141. doi:10.1038/s44321-024-00162-7
46. Liu C-C, Zhao J, Fu Y, et al. Peripheral apoE4 enhances Alzheimer's pathology and impairs cognition by compromising cerebrovascular function. *Nat Neurosci*. 2022;25:1020-1033. doi:10.1038/s41593-022-01127-0
47. Zeng P-M, Sun X-Y, Li Y, et al. Thymosin beta 4 as an Alzheimer disease intervention target identified using human brain organoids. *Stem Cell Rep*. 2025;20:102601. doi:10.1016/j.stemcr.2025.102601
48. TCW J, Qian Lu, Pipalia NH et al. Cholesterol and matrisome pathways dysregulated in astrocytes and microglia. *Cell*. 2022;185:2213-2233 e2225. doi:10.1016/j.cell.2022.05.017
49. Shi Y, Yamada K, Liddelow SA, et al. ApoE4 markedly exacerbates tau-mediated neurodegeneration in a mouse model of tauopathy. *Nature*. 2017;549:523-527. doi:10.1038/nature24016
50. Audrain M, Haure-Mirande J-V, Mleczko J, et al. Reactive or transgenic increase in microglial TYROBP reveals a TREM2-independent TYROBP-APOE link in wild-type and Alzheimer's-related mice. *Alzheimer's & Dementia*. 2021;17:149-163. doi:10.1002/alz.12256
51. Haure-Mirande J-V, Audrain M, Fanutza T, et al. Deficiency of TYROBP, an adapter protein for TREM2 and CR3 receptors, is neuroprotective in a mouse model of early Alzheimer's pathology. *Acta Neuropathol*. 2017;134(5):769-788. doi:10.1007/s00401-017-1737-3
52. Huang Y, Wang M, Ni H, et al. Regulation of cell distancing in periplaque glial nets by Plexin-B1 affects glial activation and amyloid compaction in Alzheimer's disease. *Nat Neurosci*. 2024;27:(8):1489-1504. doi:10.1038/s41593-024-01664-w
53. Wang, M, Li A, Sekiya M, et al. Transformative network modeling of multi-omics data reveals detailed circuits, key regulators, and potential therapeutics for Alzheimer's disease. *Neuron*. 2020;8:S0896-6273. doi:10.1016/j.neuron.2020.11.002
54. Zhang R, Xu X, Yu H, Xu X, Wang M, Le W. Factors influencing Alzheimer's disease risk: whether and how they are related to the APOE genotype. *Neuroscience Bulletin*. 2022;38:809-819. doi:10.1007/s12264-021-00814-5
55. Zhou X, Chen Yu, Mok KY, et al. Non-coding variability at the APOE locus contributes to the Alzheimer's risk. *Nat Commun*. 2019;10:3310. doi:10.1038/s41467-019-10945-z
56. Dehghani, N, Bras, J, Guerreiro, R. How understudied populations have contributed to our understanding of Alzheimer's disease genetics. *Brain*. 2021;144:1067-1081. doi:10.1093/brain/awab028

SUPPORTING INFORMATION

Additional supporting information can be found online in the Supporting Information section at the end of this article.

How to cite this article: Yu G, Thorpe A, Zeng Q, et al. Single-cell transcriptomic analysis reveals *APOE* genotype-dependent sex differences in Alzheimer's disease. *Alzheimer's Dement*. 2026;22:e71463. https://doi.org/10.1002/alz.71463